JOURNAL OF GEOPHYSICAL RESEARCH, VOL. 114, C00A14, doi:10.1029/2008JC005084, 2009

Seasonal and interannual variability of downwelling in the Beaufort Sea

Jiayan Yang[1]

Received 15 August 2008; revised 7 August 2009; accepted 2 September 2009; published 11 December 2009.

[1] In this paper, we examine the seasonal and interannual to decadal variability of oceanic downwelling in the Beaufort Sea. The surface wind stress is the primary driver for variability in the upper Arctic Ocean and sea ice. The seasonal variability of the surface wind over the western Arctic is strongly influenced by a high sea level pressure center that emerges in the fall and diminishes in the summer. The wind stress and sea ice velocity are both anticyclonic from fall to spring and thus force an upwelling along the Alaskan and Canadian coast and downwelling in the interior Beaufort Sea. The upwelling and downwelling varied significantly on the interannual to decadal time scales from 1979 to 2006. There was no significant correlation between the upwelling/downwelling rate in the Beaufort Sea and the Arctic Oscillation index over this 28 year period. The coastal upwelling and interior downwelling in the Beaufort Sea had gradually intensified from 1979 to 2006. This change was almost entirely due to the increase in sea ice velocity according to three additional sensitivity calculations. The anticyclonic ice velocity over the western Arctic Ocean accelerated in the 28 year period, and the acceleration was not driven solely by the wind stress. The geostrophic wind condition was actually similar between 1979–1986 and 1997–2004. However, the ice velocity was much greater in the latter period. We hypothesize that the change in ice dynamics (thinner and less areal coverage) was responsible for the change of ice velocity.

Citation: Yang, J. (2009), Seasonal and interannual variability of downwelling in the Beaufort Sea, *J. Geophys. Res.*, *114*, C00A14, doi:10.1029/2008JC005084.

1. Introduction

[2] The surface wind and sea ice motion are predominantly anticyclonic over the western Arctic Basin in association with a high sea level pressure (SLP) center from fall to spring. They weaken in the summer as the high SLP center retreats or are replaced by a low SLP center. The oceanic Ekman layer responds directly to such changes in the atmosphere and sea ice. Strong upwelling prevails along the Alaskan and Canadian coasts while downwelling occurs in the interior Beaufort Sea [*Yang*, 2006; *Yang and Comiso*, 2007]. The convergence of the Ekman transport and downwelling is important in maintaining the large reservoir of freshwater in the Beaufort Sea [*Hakkinen and Proshutinsky*, 2004]. However, little is known about interannual changes in the Arctic Ocean's upwelling and downwelling. Significant changes have been detected in every climate variable that affect the oceanic state [e.g., *Comiso et al.*, 2003; *Overland et al.*, 2008; *Steele et al.*, 2008; *Stroeve et al.*, 2008; *Nghiem et al.*, 2007]. For instance, the sea ice concentration in the summer has decreased gradually in the last 30 years in the era of satellite passive microwave observations [*Comiso and Parkinson*, 2004]. Ocean responses to changes in atmosphere and sea ice are less clear due to a lack of basin-wide and long-term observations. In this study, we will examine the response in the oceanic Ekman layer, including upwelling (divergence of the Ekman transport), to seasonal and interannual changes in the Arctic atmosphere and sea ice. We chose to focus on the Ekman layer dynamics which, from the perspective of physical oceanography, is the most fundamental process from where a more complete three dimension circulation can be examined.

[3] The surface wind stress is the only variable that is required for computing the Ekman transport in an ice-free ocean [*Hellerman and Rosenstein*, 1983]. In the partially ice-covered Arctic Ocean, however, the sea-surface stress consists of both air-water and ice-water stresses, and their partition in each grid depends on the sea ice concentration. The ice-water stress is usually computed by using sea ice velocity. The ice velocity data in the Arctic had been inferred from geostrophic wind [*Colony and Thondike*, 1984] or from positioning a number of sparsely distributed drifting buoys [*Rigor*, 2002]. A lack of high-resolution and good-quality measurements of ice motion was probably attributable to the lack of a basin-wide calculation of the Arctic Ekman transport and upwelling. This situation changed when new capability was developed in retrieving ice motion information from measurements made by satellite passive microwave sensors [*Kwok et al.*, 1998; *Fowler*, 2003].

[1]Department of Physical Oceanography, Woods Hole Oceanographic Institution, Woods Hole, Massachusetts, USA.

0148-0227/09/2008JC005084$09.00

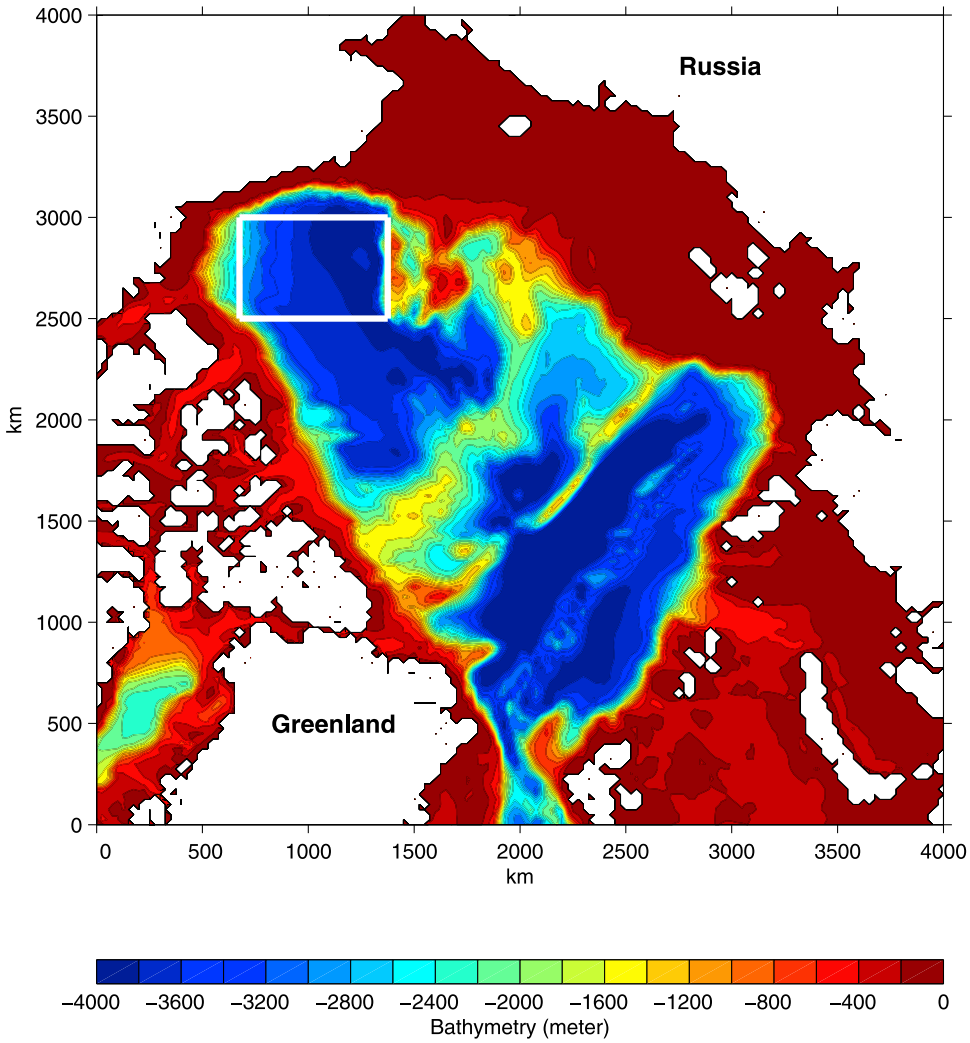

Figure 1. The bathymetry of the Arctic Basin. The data grid size is 25 km over the whole domain shown. We will concentrate our analyses of the interior Beaufort Sea in the area within the white box.

[4] A basin-wide calculation of the Ekman transport and upwelling was made recently by using the newly available ice motion data [*Yang*, 2006]. It has been used in explaining some observed seasonal changes in the upper Arctic Ocean [*Yang and Comiso*, 2007]. In this study, we will quantify the seasonal and interannual to decadal variability of downwelling in the Beaufort Sea from 1979 to 2006, and examine its relationship with atmospheric and sea ice variables, whose variability have been addressed in numerous previous studies [e.g., *Walsh et al.*, 1996; *Parkinson et al.*, 1999; *Thompson and Wallace*, 1998; *Proshutinsky and Johnson*, 1997; *Dickson et al.*, 2000; *Johnson et al.*, 1999; *Comiso et al.*, 2003]. The data sources will be described in section 2. In section 3, we will discuss downwelling variability and its relation to sea ice and atmospheric changes. A summary will follow in section 4.

2. Data Sources and Methodology

[5] The data sources and the methodology used in our calculations were described by *Yang* [2006], and so will be summarized only briefly here. The bathymetry of the Arctic basin is shown in Figure 1. The model uses the 25 km Equal-Area Scalable Earth Grid (EASE-Grid) that the National Snow and Ice Data Center (www.nsidc.org) uses for distributing many products. The direct observation of surface wind stress is extremely scarce in the Arctic. So we will follow the procedure adopted by the Arctic Ocean Model Intercomparison Project (AOMIP) [*Proshutinsky et al.*, 2001] to compute surface wind stress using the geostrophic wind. The sea level pressure (SLP) data from the International Arctic Buoy Program (IABP) [*Rigor*, 2002] are used to calculate the surface geostrophic wind, which is then converted to a 10 m surface wind by using an empirical formula [*Proshutinsky and Johnson*, 1997]. Following the AOMIP procedure, the 10 m surface wind vector (u_s, v_s) is computed using the following equations:

$$u_s = 0.8\left(u_g \cos 30^\circ - v_g \sin 30^\circ\right)$$
$$v_s = 0.8\left(u_g \cos 30^\circ + v_g \sin 30^\circ\right), \quad (1)$$

where (u_g, v_g) are geostrophic wind components. The bulk formulae are used to compute the wind stress, i.e.,

$$\vec{\tau}_{air-water} = \rho_{air} C_d |\vec{u}_s| \vec{u}_s, \quad (2)$$

where ρ_{air} = 1.25 kg m^{-3} is the air density, C_d = 0.00125 is the drag coefficient. The IABP data are distributed in the spherical coordinate and are interpolated optimally to the EASE-Grids for this study. The ice velocity data were derived from using SMMR, SSM/I, AVHRR data and positioning drifting buoys [*Fowler*, 2003] for the period from 1978 to 2006. The original ice velocity data were already gridded on the 25 km EASE-Grids and so no interpolation is needed. We have followed the AOMIP procedure for the calculation of the ice-water stress

$$\vec{\tau}_{ice-water} = \rho_{water} C_{iw} |(\vec{u}_{ice} - \vec{u}_{ocean})| (\vec{u}_{ice} - \vec{u}_{ocean}), \quad (3)$$

where ρ_{water} is the water density, C_{iw} = 0.0055 is the ice-water drag coefficient [*Hibler*, 1980], $\vec{u}_{ice}$ is the ice motion vector from *Fowler* [2003] and $\vec{u}_{ocean}$ is the upper layer ocean current velocity which, in our calculation, is set by the Ekman velocity $\vec{u}_{Ekman}$. The total stress on each grid is then calculated by

$$\vec{\tau} = \alpha \vec{\tau}_{ice-water} + (1 - \alpha)\vec{\tau}_{air-water}, \quad (4)$$

where α is the fraction of the grid that is covered by sea ice, $\vec{\tau}_{ice\text{-}water}$ and $\vec{\tau}_{air\text{-}water}$ are the ice-water and air-water interfacial stresses, respectively. The satellite passive microwave sea ice concentration data [*Comiso*, 1995] is used for determining α. Using the total stress, we can now calculate the Ekman layer velocity by using the textbook Ekman layer equation [e.g., *Pond and Pickard*, 1983]

$$-fv_{Ekman} = \frac{\tau^x}{\rho D_E} \quad \text{and} \quad fu_{Ekman} = \frac{\tau^y}{\rho D_E}, \quad (5)$$

where D_E = 20 m is the Ekman layer depth (the Arctic Ocean Ekman depth, according to observation by *Hunkins* [1966], is about 18 m). The Ekman velocity (u_{Ekman}, v_{Ekman}) in (5) is the vertically averaged velocity within the Ekman layer. Since the stress and the Ekman velocity are dependent on each other, equations (2)–(5) are solved iteratively. The upwelling and downwelling are induced by the divergence and convergence of the Ekman transport, and can be readily obtained once the Ekman transport is computed

$$w = \nabla \cdot (D_E \vec{u}_{Ekman}). \quad (6)$$

On each land grid, the Ekman transport is set to be zero, so there is usually a large convergence or divergence on any sea grid next to the land. The method used here is probably overly simplified for calculating coastal upwelling since it does not consider any bathymetric effect. In addition, the method obviously becomes invalid in very shallow areas where the surface and bottom Ekman layers may overlap each other. In the interior Beaufort Sea, which is the focus of this study, equations (5) and (6) should be appropriate for estimating the Ekman transport and upwelling on the zeroth order. We should note that the Ekman layer depth D_E does not directly affect Ekman transport $D_E(u_{Ekman}, v_{Ekman})$, and upwelling, described by (5) and (6). But it does affect the calculation of the ice-water stress which, according to (3), depends on the velocity, not the transport of the Ekman layer. Setting D_E = 20 m uniformly over the whole model domain is likely a source of bias for our calculation. We have experimented with different values of D_E and the results were virtually the same because the Ekman velocity is usually considerably smaller than the ice velocity. Another source of error is due to the neglect of the non-Ekman velocity in the surface velocity in equation (3). The geostrophic velocity could be large in frontal regions or in places with strong jets. While these problems may not necessarily be unique in the ice-covered regions, they nevertheless contribute to the overall bias in our calculation.

[6] In this study, we use the daily fields of the three variables to compute the daily Ekman transport and the upwelling rate according to equations (5) and (6). Using the monthly mean forcing fields would result in biases due to the nonlinearity of the bulk formulas (2) and (3). Once the daily upwelling was computed, the monthly mean upwelling was then calculated by simply averaging the daily field within each month.

3. Variability of Upwelling in the Beaufort Sea

[7] This study focuses mainly on changes and trends in the Beaufort Sea where the downwelling is very strong. Here, we start with an examination of the seasonal cycle and its relationship to the atmospheric and sea ice changes. The ultimate driver of the seasonality is the atmosphere. Sea ice covers the whole Arctic in the winter months and retreats from the southern boundary in the summer (Figure 2a for the 28 year climatology). In the summer, there are large areas that are ice free along the Canadian, Alaskan and Russian coasts, and they are exposed to the direct wind stress forcing. The change in the atmosphere is dictated by the seasonality of the SLP (Figure 2b). A high SLP center emerges over the western Arctic in the late fall, typically around September–October, intensifies in the early winter, and persists through the winter into the spring. It induces an anticyclonic wind which then forces sea ice to move likewise. The wind and ice velocity are particularly strong along the southern Beaufort and Chukchi Seas (Figure 2c). Driven by the easterly stress exerted by the anticyclonic wind and ice velocity, the Ekman transport is directed offshore along the Alaskan and Canadian coast (Figure 2d). This results in strong coastal upwelling and interior downwelling in the Beaufort and Chukchi Seas (Figure 2e). During the late spring and summer, the wind and ice velocity are typically weak, and so the upwelling during this period is weak as well. The salinity at the end of the summer is particularly low along the Alaskan and Canadian coast as a result of the summer melt and the accumulation of spring and summer runoff. The offshore Ekman transport in the fall and winter moves the coastal low salinity to the interior Beaufort Sea and the Ekman pumping there pushes the halocline deeper. This seasonal cycle of Ekman transport results in an unexpected salinity change, as observed by buoys, that salinity in the upper Beaufort Sea was lower in the winter than in the summer [*Yang and Comiso*, 2007].

[8] Seasonal changes of surface wind and ice velocity are large in the Beaufort Sea and the oceanic response is great. In a recent analysis of in situ observation, *Pickart et al.* [2009] showed that upwelling over the Beaufort Sea shelf and slope is strongly affected by the intensity and trajectories of Pacific-born storms. To better represent the overall

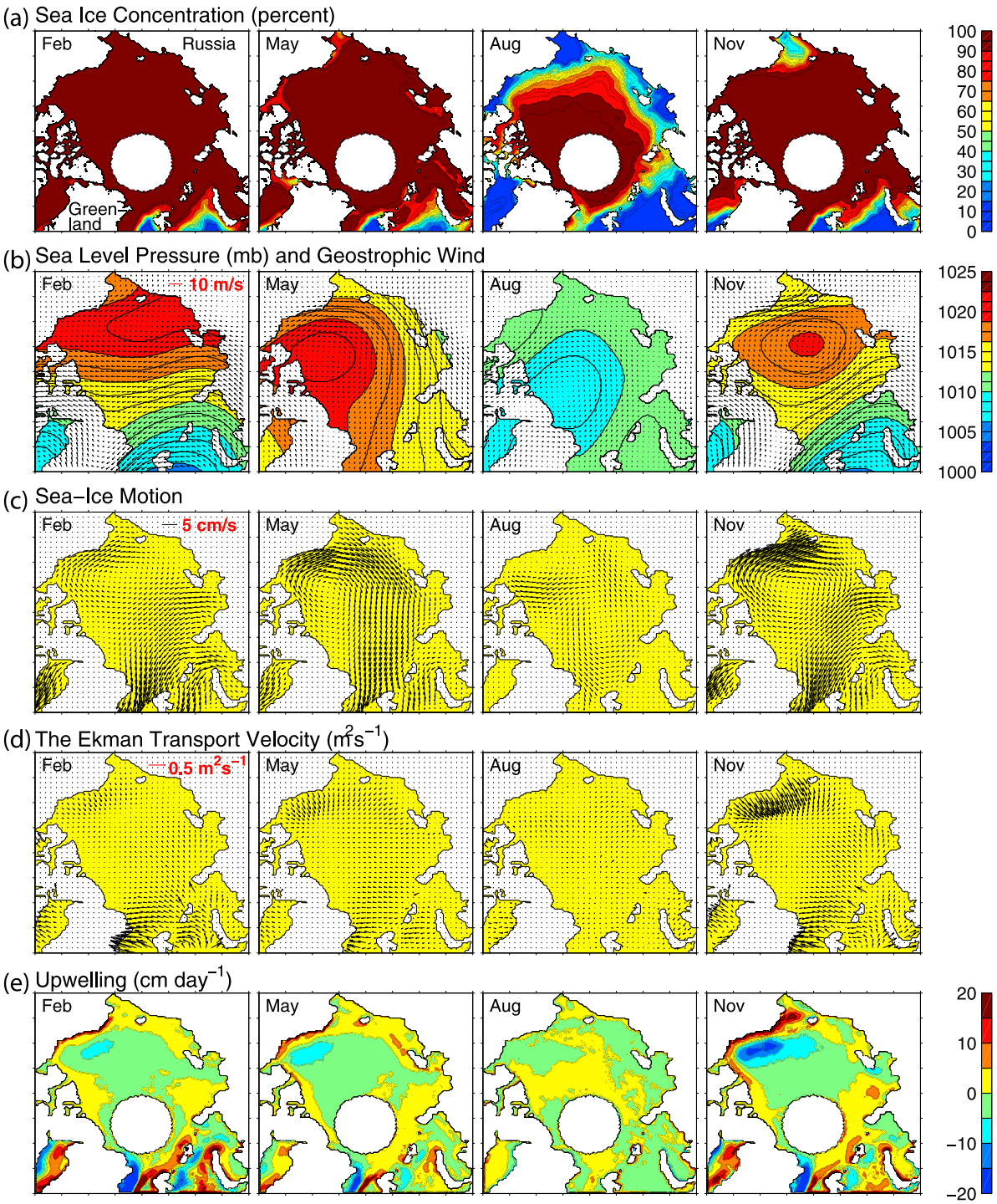

Figure 2. The climatological seasonal variability of (a) sea ice concentration, (b) SLP and geostrophic wind, (c) sea ice velocity, (d) Ekman transport, and (e) upwelling. The data used here are based on 28 year (1979–2006) daily fields.

seasonality over the broad Beaufort Sea interior, we choose to average the upwelling rate over a large area in the Beaufort Sea, shown within the white box in Figure 1. The 28 year (1979–2006) monthly climatology shows a robust seasonal variability (Figure 3a). The downwelling (negative value) prevails in all 12 months in the interior Beaufort Sea. The maximum downwelling occurs in November and December, with a rate over 8 cm/d. The downwelling becomes weaker later in the winter between March and April, and restrengthens in May. This resurgence in May is related to the seasonal reintensification of the high SLP center over the western Arctic as discussed by *Yang* [2006]. The downwelling remains weak during the summer months. The seasonal change of sea ice coverage may have played a role in the ocean's response to wind stress forcing. For example, the downwelling rate between January and

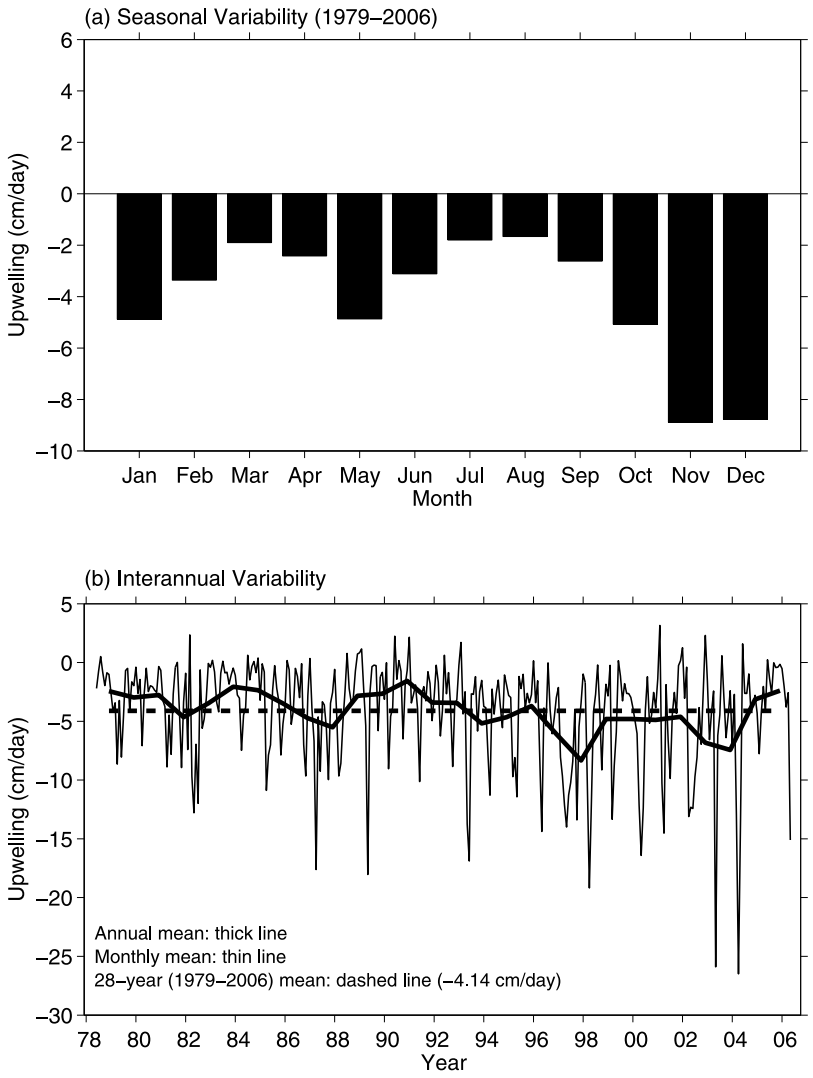

Figure 3. (a) The monthly variability of the interior Beaufort Sea upwelling rate over the area inside the white box shown in Figure 1 and averaged over a 28 year period between 1979 and 2006. (b) The 28 year time series of the monthly upwelling. (Units are cm/d with positive for upwelling and negative for downwelling.)

March is relatively weaker than for the period between October and December. The surface wind remains robustly anticyclonic in the first 3 months of the year. The reduction of the downwelling after January is likely due to the nearly 100% ice coverage which not only shields the ocean from a direct wind stress forcing but also seems to slow down the ice velocity (Figure 2c), likely due to internal ice dynamics. Such a transition was observed by a moored array deployed across the Beaufort shelf break and slope near 152W between the fall of 2002 and winter of 2003 [*Pickart et al.*, 2009]. The responses of both the ice velocity and upwelling to a storm-induced easterly wind were prompt and profound before the mooring site was 100% covered by sea ice. The response to storms of similar strength was much reduced once the area was completely covered by sea ice.

[9] The downwelling rate averaged 4.14 cm/d (over the white box shown in Figure 1) between January 1979 and December 2006 (dashed line in Figure 3b, negative value for downwelling and positive value for upwelling). There are, however, considerable variations on interannual to decadal time scales over this 28 year period. The downwelling in the summer was weak and varied within ±5 cm/d. The more profound change occurred in the fall and early winter. There was a clear trend that the winter downwelling had increased significantly in this region. For example, the winter downwelling reached as great as 25 cm/d in 2003 and 2004 as compared with a more typical 10 cm/d in the early 1980s (Figure 3b).

[10] The leading mode of atmospheric variability in the northern hemisphere is the Arctic Oscillation (AO) [*Thompson and Wallace*, 1998]. It is defined by the first EOF mode of the SLP variability. Figure 4 shows the time series of the AO index from 1979 to 2006 (solid line for the annual mean and dashed line for the winter months). Over this 28 year period, the AO index was high during the period of 1988–1994, and was lower before and after this period. The annually mean downwelling rate in the Beaufort Sea (bold line in Figure 3) was similar between the periods of 1979–1986 and 1988–1994 even though the AO index was

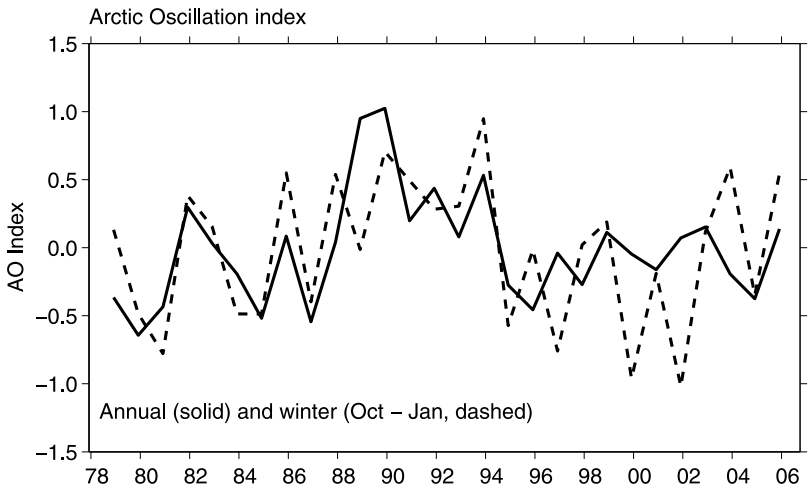

Figure 4. The Arctic Oscillation index [*Thompson and Wallace*, 1998]. There was not an obvious correlation between the AO index and the upwelling in the Beaufort Sea shown in Figures 2 and 3.

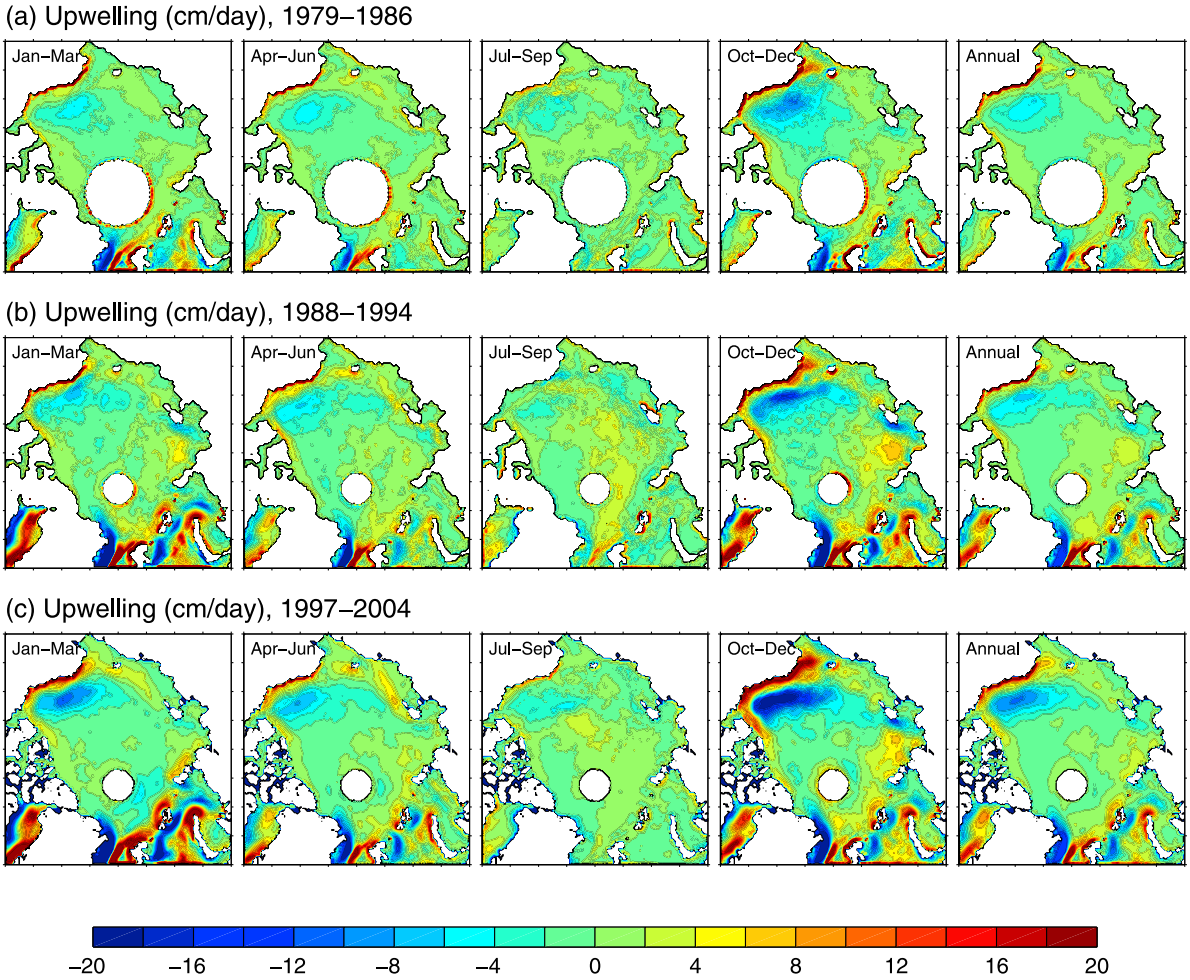

Figure 5. The upwelling (positive) and downwelling (negative) for the three periods that were chosen for this study: (a) 1979–1986, (b) 1988–1994, and (c) 1997–2004. Note that the upwelling/downwelling in the Beaufort Sea had increased noticeably over this 28 year period. The change was most pronounced in the fall season.

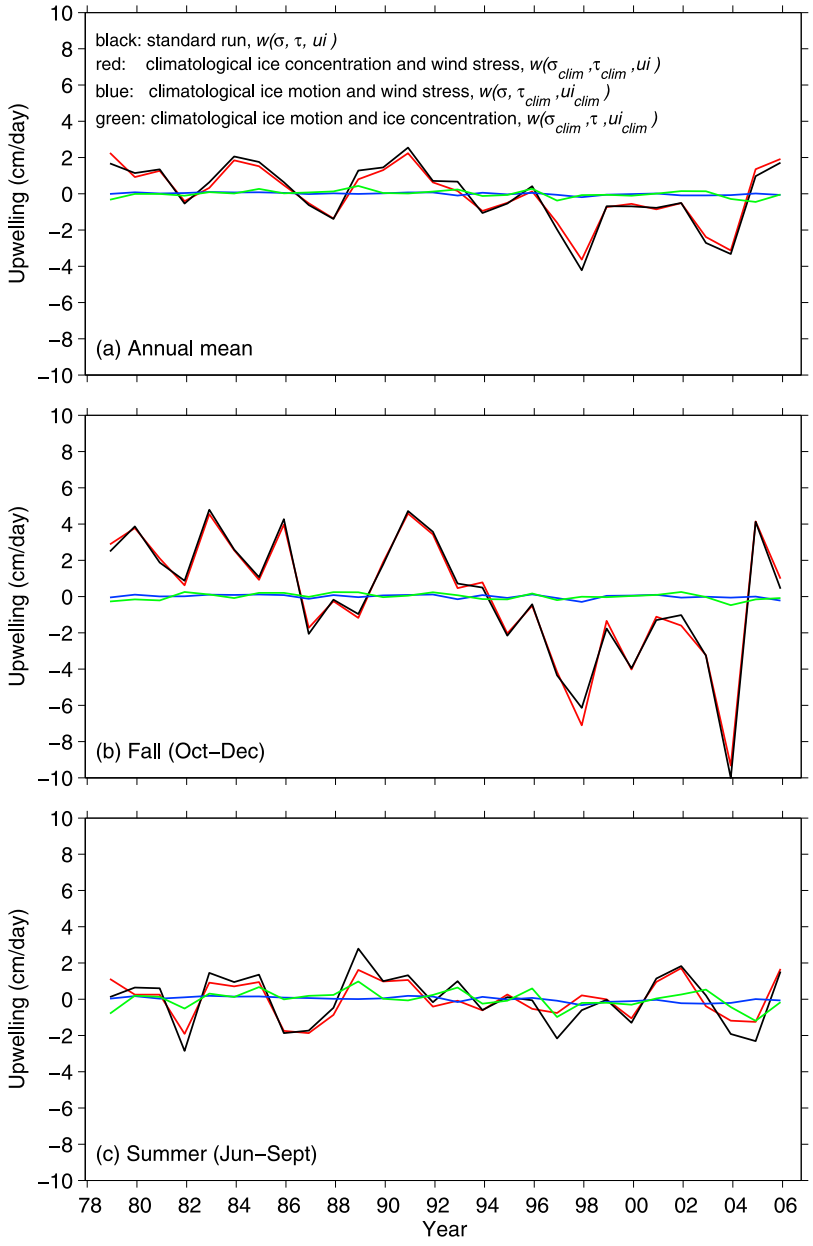

Figure 6. The anomalous upwelling rate. (a) The annual mean upwelling rate, (b) the fall season upwelling, and (c) the summer season upwelling. Note that the change occurred more significantly in the fall months (black lines for the standard calculation, red lines for variation due to ice velocity, blue lines for variations due to ice concentration, and green lines for variations due to air-water stress). The interannual to decadal changes were clearly dominated by changes induced by sea ice velocity.

considerably different (Figure 4). In the 1997–2004 period, however, the downwelling was larger than in the 1980s and early 1990s while the AO index was rather similar to that in 1979–1986. Obviously, there was no significant correlation between the downwelling rate in the Beaufort Sea and the AO index over this 28 year period.

[11] The surface wind stress, which drives the sea ice velocity and the ocean, is related intimately to the geostrophic wind, which itself is derived from the SLP. Since the AO represents the leading mode of SLP variability, it is quite puzzling why there was no significant correlation between the upwelling and AO index. It is clear, however, that the downwelling variability must be related to the combination of three forcing variables according to the Ekman model. In the following analyses, we will examine these variations during the three periods discussed above, namely, 1979–1986, 1988–1994, and 1997–2004. The AO index was high in the 1988–1994 period. We are interested in oceanic changes before, during and after this period of high AO index.

[12] The basin-wide upwelling (positive) and downwelling (negative) during the three periods are shown in Figure 5.

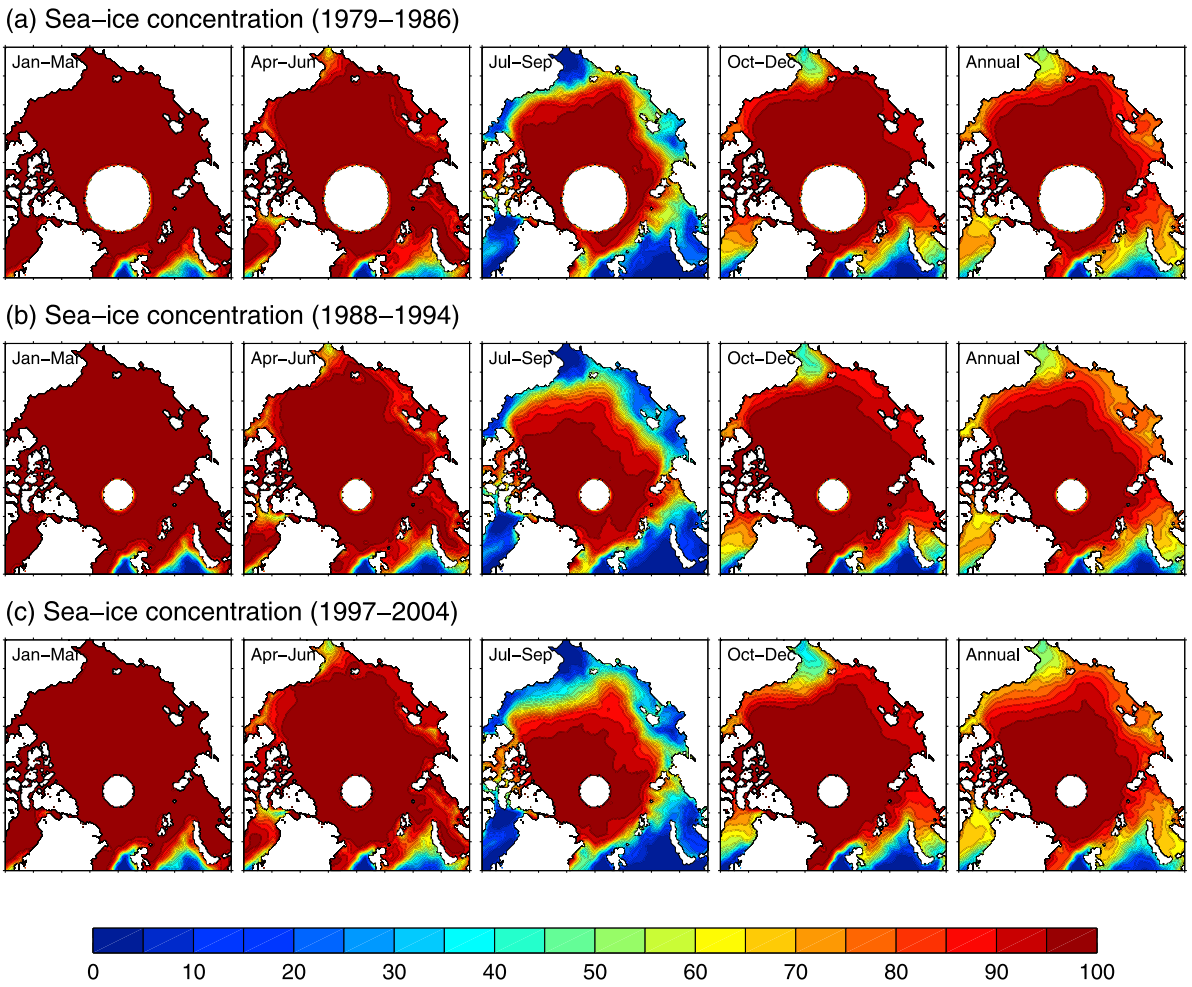

Figure 7. The sea ice concentration for the periods of (a) 1979–1986, (b) 1988–1994, and (c) 1997–2004. The largest changes occurred in the summer and fall.

Over our study area in the Beaufort Sea (marked by a white box in Figure 1), the downwelling was weak in both spring (April–June) and summer (July–September) in all three periods. The winter downwelling (January–March) in the Beaufort Sea was stronger than that in the summer and spring in all periods. So the seasonality in each period was consistent with the 28 year climatology shown earlier. It is noted that the downwelling in the Beaufort Sea had strengthened considerably over these three periods. The maximum downwelling rate in the Beaufort Sea increased from about 5 cm/d in 1979–1986 to more than 10 cm/d in 1997–2004. The coastal upwelling along the Alaskan and Canadian coast had also strengthened. The strongest downwelling and largest interannual changes occurred in the fall between October and December. The change in the annual mean field was largely due to the strengthening of w in the fall.

[13] The anomalous downwelling (28 year mean removed) averaged over the white box area in Figure 1 is indicated by the black lines in Figure 6. In this 28 year period, the summer downwelling was weaker and showed no obvious trend (Figure 6c). In contrast, the downwelling in fall not only varied interannually, but also had strengthened considerably (Figure 6b). The change in the annual mean w (Figure 6a) was dictated by winter variability. Which forcing variable was responsible for the changes? Three additional calculations were made to answer this question. In the first sensitivity experiment, the sea ice velocity and wind stress in equations (1)–(6) were replaced by the daily climatologies averaged between 1979 and 2006. The interannual variation in the forcing field, equation (4), was solely due to changes in the sea ice concentration. The downwelling anomaly in the Beaufort Sea was very small (blue lines in Figure 6), even in the summer when sea ice coverage varied most profoundly. The best observed, and perhaps the most significant change that occurred in the Arctic climate system in the last 30 years, was the steady decline of summer sea ice coverage. How can this insensitivity of downwelling to changes in ice concentration be explained?

[14] We plotted the seasonal variability of the sea ice concentration in the three periods (Figure 7). As expected, the greatest changes occurred in the summer months from June to August when the ice cover is typically at its seasonal minimum. Figure 7 shows a familiar pattern of a steady decline of summer sea ice coverage over the Arctic basin in the last three decades. In summer, the surface wind and ice velocity are both typically weak, and thus the downwelling in the Beaufort Sea is usually at its seasonal minimum (Figure 3a). The ice concentration is used in our model only

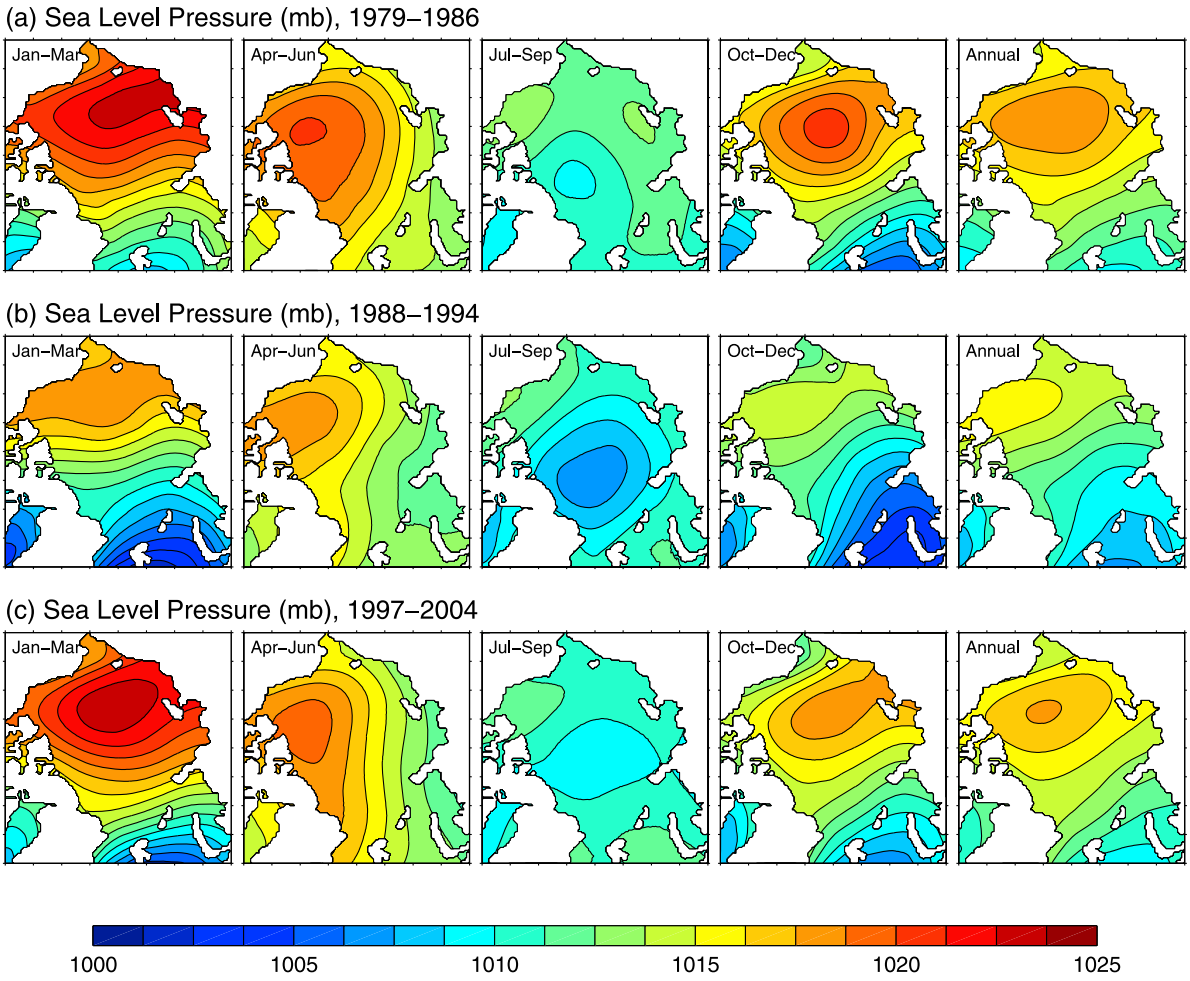

Figure 8. The seasonal variability of SLP for the three periods chosen in this study: (a) 1979–1986, (b) 1988–1994, and (c) 1997–2004. Note that the seasonal variability was very similar between 1979 and 1986 and 1997–2004 when the AO index was low.

for partitioning the ice-water and air-water stresses. The surface wind and ice motion are both sluggish in the summer, and consequently the total surface stress, as defined by equation (4), is small (compared with fall and winter) regardless of the state of sea ice coverage. In the winter and spring, on the other hand, the whole Arctic is nearly 100% covered by sea ice with virtually no interannual changes in the area of our study (January–March and April–June in Figure 7). Not surprisingly, the sea ice concentration plays no direct role in interannual and decadal changes of w during these seasons. The Beaufort Sea is mostly, but not yet completely covered by sea ice from October to December. But the difference of ice concentration over the three periods was rather small (October–December in Figure 7). This may well explain the small contribution to the overall downwelling rate. In summary, the variability of sea ice concentration was not directly responsible for the large change of oceanic downwelling in the Beaufort Sea. The ice concentration, however, does affect the response of the ice velocity to wind stress forcing. This will be discussed later when we examine the role of ice velocity.

[15] In the second sensitivity experiment, the ice concentration and ice velocity were replaced by daily climatologies. So the interannual variation in the forcing field is solely due to changes in the air-water stress. The green lines in Figure 6 show the anomalous w in the Beaufort Sea from 1979 to 2006. Like the ice concentration, the surface wind stress has virtually no direct impact on the interannual and decadal change in w. The only detectable variation occurred in the summer (green line in Figure 6c). The lack of the contribution to w does not mean that the atmosphere did not vary over this 28 year period. Figure 8 shows the SLP in four seasons during the periods of 1979–1986, 1988–1994, and 1997–2004. The seasonal variability of SLP was quite similar between 1979–1986 and 1997–2004 when the AO index was low. The seasonal evolution was significantly different during the period of 1988–1994 when the AO was high. The high SLP center in winter over the western Arctic was substantially weakened. The SLP contours aligned in a band structure across the basin (January–March in Figure 8b). Consequently, the winter became less anticyclonic. The low SLP center in summer was stronger in 1988–1994 than in the other two periods. The wind stress is felt directly by the ocean only when ice cover is less than 100%. The lack of the response of w to interannual and decadal variations of air-water stress in Figure 6 (green lines) in the winter, spring and even in fall is quite understandable since the Beaufort

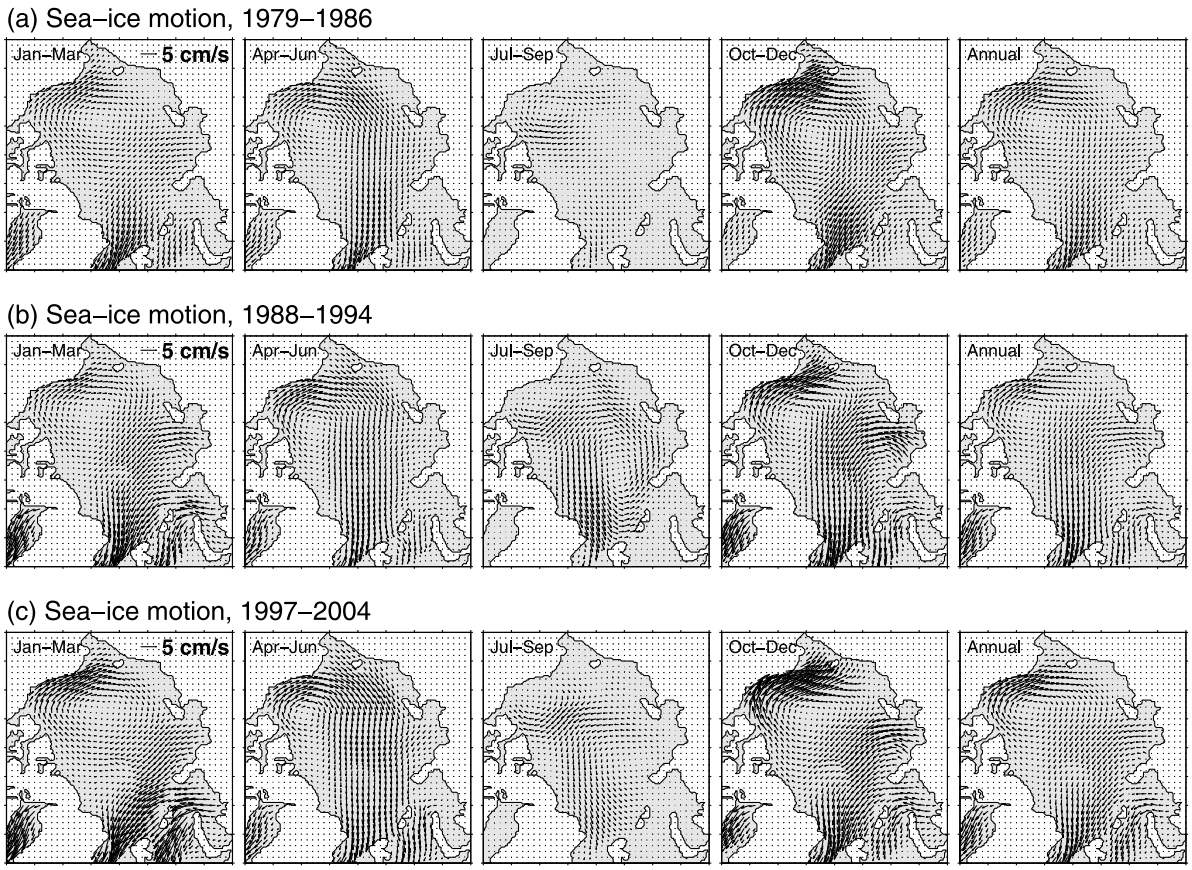

Figure 9. The sea ice velocity for (a) 1979–1986, (b) 1988–1994, and (c) 1997–2004.

Sea is almost completely shielded by sea ice, and therefore is not forced directly by wind stress. In the summer, the wind was sluggish in all three periods, and thus made only a minor impact on the downwelling.

[16] Because both the air-water stress and the ice concentration played minor roles in the interannual and decadal changes of w in the Beaufort Sea, the remaining variable, the ice velocity, must have played a leading role. In the third sensitivity experiment, the ice concentration and wind stress in equation (4) were replaced by their daily climatologies while interannually varying sea ice velocity was used. The resulted w in the Beaufort Sea (red lines in Figure 6) was nearly identical to the standard calculation (black lines).

[17] The seasonality of the ice velocity is shown in Figure 9. The pattern of ice velocity was very similar in every season for the three periods chosen for this study. Anticyclonic circulation peaked in the fall and persisted through the winter and spring. The ice velocity was small in the summer. The magnitude of the ice velocity, however, had changed significantly (Figure 10). The ice circulation had accelerated in most seasons except summer in the southern Beaufort and Chukchi Seas, where the reduction of sea ice coverage resulted in weaker averaged ice speed (the ice velocity is set to zero in the open water area). The increase in ice velocity was particularly large in the fall when the downwelling was at its seasonal maximum. The averaged ice speed in the Beaufort Sea was around 5 to 8 cm/s in the fall of 1979–1986. It increased to 6 to 10 cm/s in 1988–1994 and 8 to over 10 cm/s in 1997–2004 (July–September in Figure 10).

[18] The three sensitivity experiments clearly identify the sea ice motion as the leading cause for the interannual and decadal changes of the downwelling in the Beaufort Sea. We must point out that the wind stress is the ultimate driver of the ice velocity and thus must have played an important, though indirect, role. As Figure 8 shows, the SLP varied significantly on a decadal time scale as characterized by the Arctic Oscillation index. But the SLP was actually quite similar between 1979–1986 and 1997–2004 when the AO index was low. The speed of geostrophic wind, which is linearly proportional to the surface wind speed according to equation (1) in our model, shows no significant difference between these two periods (Figure 11). Another interesting feature is that the wind was nearly as strong in the winter (January–March) as in the fall (October–December) (Figure 11). Yet the ice velocity, however, decelerated from the fall to the winter (Figure 10). The wind stress was the main driver during the seasonal spin-up of the anticyclonic sea ice circulation in the fall. But the wind stress in the winter, though as strong as in the fall, was overwhelmed by internal ice stress and/or oceanic drag once the ice became thicker and more tightly packed. Could this explain the decadal changes? Various studies have shown that the Arctic pack ice has thinned [*Rothrock et al.*, 1999]. The sea ice concentration in the fall and summer had also decreased substantially (Figure 7). It is possible that the ice velocity became more responsive to the wind stress forcing when the ice was thinner in 1997–2004, and thus the ice speed increased, even though the wind stress remained unchanged. This scenario is plausible and seems to be supported by

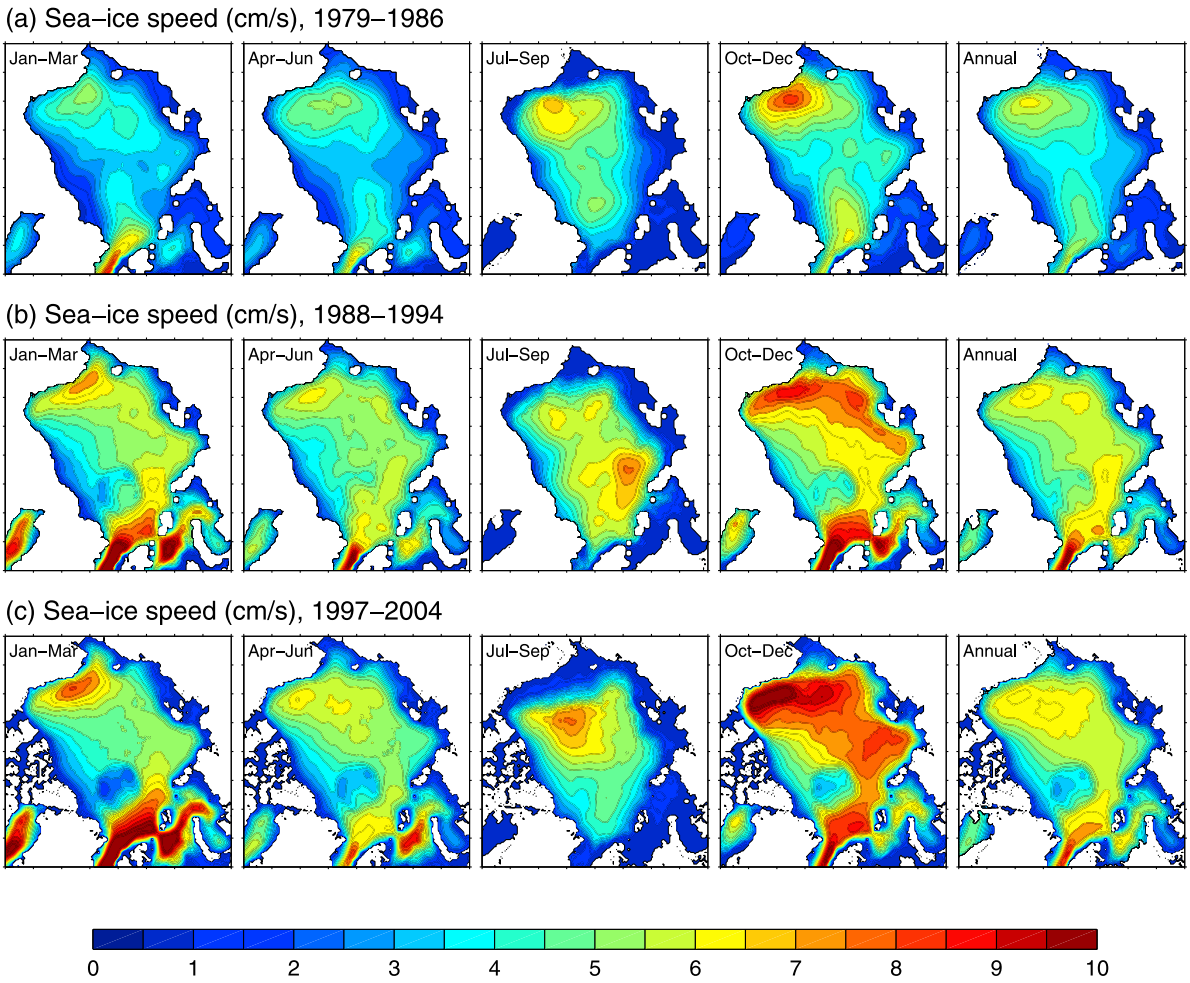

Figure 10. The speed of ice motion for (a) 1979–1986, (b) 1988–1994, and (c) 1997–2004. The ice velocity had accelerated in this 28 year period. It is interesting to note that the ice speed was much faster in 1997–2004 than in 1979–1986 even though the SLP and wind speed (Figure 11) were similar in these two periods.

recent in situ observation in the Beaufort shelf break and slope [*Pickart et al.*, 2009]. Data collected by an array of moorings across the Beaufort shelf break and slope near 152W showed that the ice speed was much larger and upwelling was stronger before the area was covered 100% by sea ice. The responses in ice speed and upwelling were reduced even under similar wind stress forcing once the area was completely covered by ice.

[19] We acknowledge here that the linkage between ice speed and ice coverage, and thickness is speculative in nature. A conclusive confirmation, however, needs to involve sea ice modeling. This is beyond the scope of this study. We hope this would motivate modeling studies, whereby a more robust linkage can be established. We would like to point out that a main source of error in our calculation is the use of constant ice-water drag coefficient. The momentum transfer between sea ice and water clearly depends on the underneath roughness of sea ice. However, there is no basin-wide data of ice roughness from observation. This again can only be handled by sea ice models with sophisticated treatments of the turbulent boundary layer beneath the sea ice. One possibility is that the overall ice roughness decreased as the sea ice thinned. Therefore, the momentum transfer from ice to the water became less efficient even if the ice velocity became faster in the more recent decade. The offset of an increasing ice speed by a lessening roughness would reduce the trend of a strengthening oceanic upwelling/downwelling in the Arctic Ocean.

[20] We would like to revisit the issue of lacking AO correlation with the downwelling in the Beaufort Sea. The AO represents a leading mode of the SLP variability and of the change of geostrophic wind. But the response in ice velocity, which is the main driver of the upwelling, to wind stress forcing depends on the ice thickness and concentration as we discussed above. The ice speed was very different between 1979–1986 and 1997–2004 even though the AO index and geostrophic wind were similar in these two periods. So we hypothesize that the change of ice velocity's response to wind stress was attributable to the lack of correlation between the AO index and the Arctic upwelling.

4. Summary

[21] In this study, we examined the seasonal and interannual to decadal variability of the downwelling in the interior

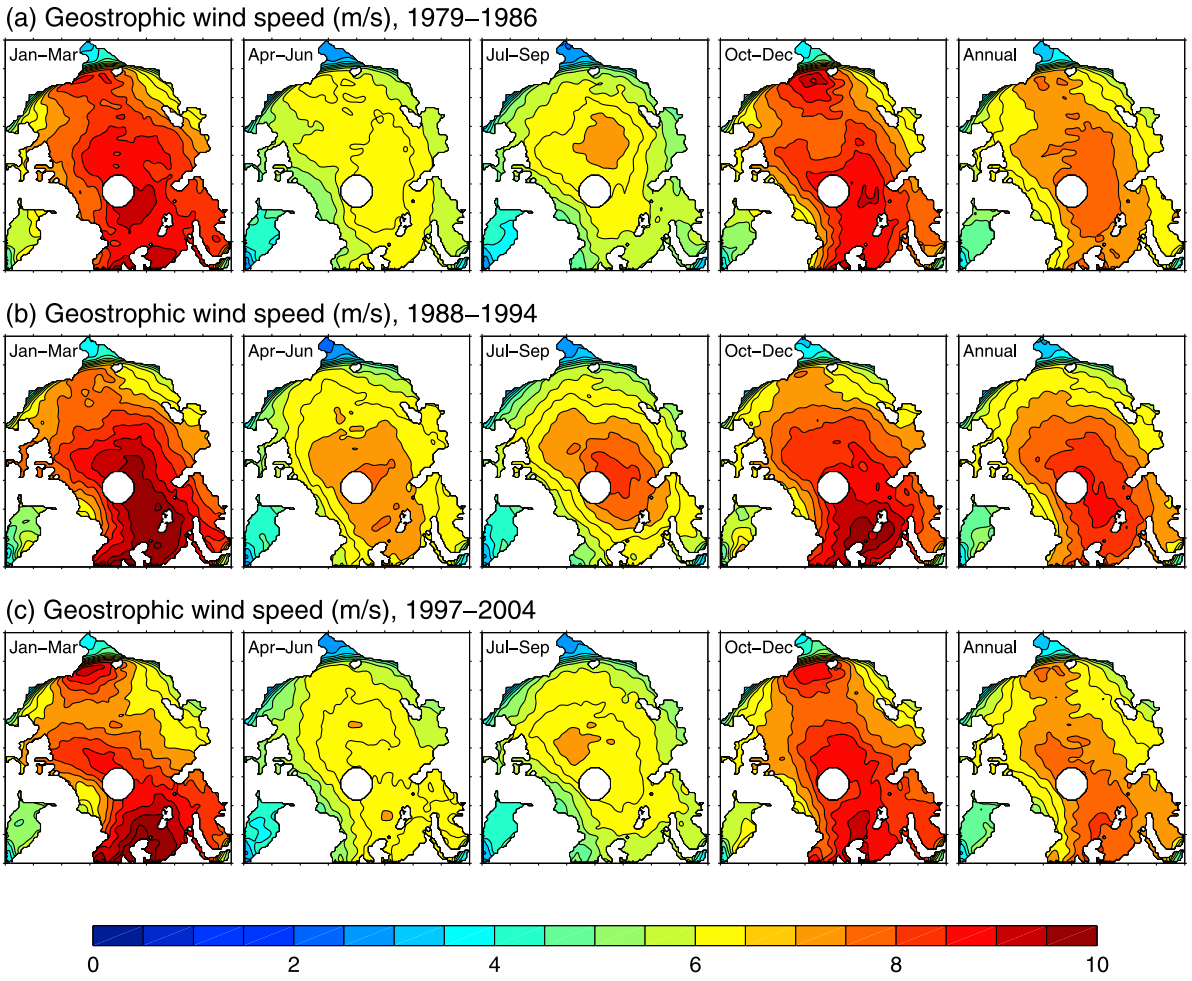

Figure 11. The speed of the geostrophic wind for (a) 1979–1986, (b) 1988–1994, and (c) 1997–2004. Unlike the ice velocity, there was no upward trend of wind speed.

Beaufort Sea. The downwelling reaches its seasonal maximum in the fall and minimum in the summer. The seasonal variability is forced by the appearance of a high SLP center from the fall to spring. The wind stress and ice velocity are both anticyclonic from fall to spring. They force an offshore Ekman transport away from the Alaskan and Canadian coasts. The transport converges in the Beaufort Sea, and results in a downwelling in all seasons. The downwelling in the Beaufort Sea varied significantly on the interannual to decadal time scales. The variation, however, was not correlated significantly with the Arctic Oscillation index. We performed three additional experiments and were able to identify that the change of sea ice velocity was mainly responsible for the variability of the downwelling. It was interesting to note that the ice velocity accelerated in the 28 year period. The acceleration was not driven solely by the wind stress. The geostrophic wind condition was actually similar between 1979–1986 and 1997–2004. But the ice velocity was much greater in the latter period. We hypothesize that the change of ice dynamics (thinner and less areal coverage) was responsible for the change of ice velocity.

[22] **Acknowledgments.** This study has been supported by the National Science Foundation's Office of Polar Program (OPP0424074 and ARC-0902090), WHOI Arctic Initiative, and NASA's Cryospheric Science Program (NNG05GN93G). The author benefits from discussion with Andrey Proshutinsky.

References

Colony, R., and A. S. Thondike (1984), An estimate of the mean field of sea ice motion, *J. Geophys. Res.*, *89*, 10,623–10,629, doi:10.1029/JC089iC06p10623.

Comiso, J. C. (1995), Remote sensing of the Arctic, in *Arctic Oceanography: Marginal Ice Zones and Continental Shelves*, *Coastal Estuarine Stud. Ser.*, vol. 49, edited by W. Smith Jr. and J. Grebmeier, pp. 1–50, AGU, Washington, D. C.

Comiso, J. C., and C. L. Parkinson (2004), Satellite-observed changes in the Arctic, *Phys. Today*, *57*(8), 38–44, doi:10.1063/1.1801866.

Comiso, J. C., J. Yang, S. Honjo, and R. A. Krishfield (2003), Detection of change in the Arctic using satellite and in situ data, *J. Geophys. Res.*, *108*(C12), 3384, doi:10.1029/2002JC001347.

Dickson, R. R., T. J. Osborn, J. W. Hurrell, J. Meincke, J. Blindheim, B. Aadlandsvik, T. Vinje, G. Alekseev, and W. Maslowski (2000), The Arctic Ocean response to the North Atlantic Oscillation, *J. Clim.*, *13*, 2671–2696, doi:10.1175/1520-0442(2000)013<2671:TAORTT>2.0.CO;2.

Fowler, C. (2003), Polar Pathfinder Daily 25 km EASE-Grid Sea Ice Motion Vectors, http://nsidc.org/data/nsidc-0116.html, Natl. Snow and Ice Data Cent., Boulder, Colo. (Updated 2007.)

Hakkinen, S., and A. Proshutinsky (2004), Freshwater content variability in the Arctic Ocean, *J. Geophys. Res.*, *109*, C03051, doi:10.1029/2003JC001940.

Hellerman, S., and M. Rosenstein (1983), Normal monthly wind stress over the World Ocean with error estimates, *J. Phys. Oceanogr.*, *13*, 1093–1104, doi:10.1175/1520-0485(1983)013<1093:NMWSOT>2.0.CO;2.

Hibler, W. D., III (1980), A dynamic and thermodynamic sea ice model, *J. Phys. Oceanogr.*, *10*, 815–846.

Hunkins, K. (1966), Ekman drift currents in the Arctic Ocean, *Deep Sea Res.*, *13*, 607–620.

Johnson, M. A., A. Y. Proshutinsky, and I. V. Polyakov (1999), Atmospheric patterns forcing two regimes of Arctic circulation: A return to anticyclonic condition?, *Geophys. Res. Lett.*, *26*, 1621–1624, doi:10.1029/1999GL900288.

Kwok, R., A. Schweiger, D. A. Rothrock, S. Pang, and C. Kottmeier (1998), Assessment of sea ice motion from sequential passive microwave observations with ERS and buoy ice motions, *J. Geophys. Res.*, *103*(C4), 8191–8213, doi:10.1029/97JC03334.

Nghiem, S. V., I. G. Rigor, D. K. Perovich, P. Clemente-Colon, J. W. Weatherly, and G. Neumann (2007), Rapid reduction of Arctic perennial sea ice, *Geophys. Res. Lett.*, *34*, L19504, doi:10.1029/2007GL031138.

Overland, J., J. Turner, J. Francis, N. Gillett, G. Marshall, and M. Tjernstrom (2008), The Arctic and Antarctic: Two faces of climate changes, *Eos Trans. AGU*, *89*(19), 177–178, doi:10.1029/2008EO190001.

Parkinson, C., D. J. Cavalieri, P. Gloersen, H. J. Zwally, and J. C. Comiso (1999), Arctic sea ice extents, areas, and trends, 1978–1996, *J. Geophys. Res.*, *104*, 20,837–20,856, doi:10.1029/1999JC900082.

Pickart, R. S., G. W. K. Moore, D. J. Torres, P. S. Fratantoni, R. A. Goldsmith, and J. Yang (2009), Upwelling on the continental slope of the Alaskan Beaufort Sea: Storms, ice, and oceanographic response, *J. Geophys. Res.*, *114*, C00A13, doi:10.1029/2008JC005009.

Pond, S., and G. Pickard (1983), *Introductory Dynamical Oceanography*, 329 pp., Pergamon Press, Oxford, U. K.

Proshutinsky, A. Y., and M. A. Johnson (1997), Two circulation regimes of the wind-driven Arctic Ocean, *J. Geophys. Res.*, *102*, 12,493–12,514, doi:10.1029/97JC00738.

Proshutinsky, A. Y., et al. (2001), Multinational effort studies differences among Arctic Ocean models, *Eos Trans. AGU*, *82*(51), 637–644, doi:10.1029/01EO00365.

Rigor, I. (2002), IABP Drifting Buoy, Pressure, Temperature, Position, and Interpolated Ice Velocity, http://nsidc.org/data/g00791.html, Natl. Snow and Ice Data Cent., Boulder, Colo.

Rothrock, D. A., Y. Yu, and G. A. Maykut (1999), Thinning of the Arctic sea ice cover, *Geophys. Res. Lett.*, *26*, 3469–3472, doi:10.1029/1999GL010863.

Steele, M., W. Ermold, and J. Zhang (2008), Arctic Ocean surface warming trends over the past 100 years, *Geophys. Res. Lett.*, *35*, L02614, doi:10.1029/2007GL031651.

Stroeve, J., M. Serreze, S. Drobot, S. Gearheard, M. Holland, J. Maslanik, W. Meier, and T. Scambos (2008), Arctic sea-ice extent plummets in 2007, *Eos Trans. AGU*, *89*(2), 13–14, doi:10.1029/2008EO020001.

Thompson, D. W. J., and J. M. Wallace (1998), The Arctic Oscillation signature in wintertime geopotential height and temperature fields, *Geophys. Res. Lett.*, *25*, 1297–1300, doi:10.1029/98GL00950.

Walsh, J. E., W. L. Chapman, and T. L. Shy (1996), Recent decrease of sea level pressure in the central Arctic, *J. Clim.*, *9*, 480–486, doi:10.1175/1520-0442(1996)009<0480:RDOSLP>2.0.CO;2.

Yang, J. (2006), The seasonal variability of the Arctic Ocean Ekman transport and its role in the mixed layer heat and salt fluxes, *J. Clim.*, *19*, 5366–5387, doi:10.1175/JCLI3892.1.

Yang, J., and J. Comiso (2007), An unexpected seasonal variability of salinity in the Beaufort Sea upper layer in 1996–1998, *J. Geophys. Res.*, *112*, C05034, doi:10.1029/2004JC002716.

J. Yang, Department of Physical Oceanography, Woods Hole Oceanographic Institution, 266 Woods Hole Rd., Woods Hole, MA 02543, USA. (jyang@whoi.edu)